Behavior of a Bose-Einstein condensate containing a large number of atoms interacting through a finite-range interatomic interaction

Tapan Kumar Das,[1] Sylvio Canuto,[2] Anasuya Kundu,[1] and Barnali Chakrabarti[3]
[1]*Department of Physics, University of Calcutta, 92 A.P.C. Road, Calcutta-700009, India*
[2]*Instituto de Física, Universidade de São Paulo, Caixa Postal 66318, 05315-970, São Paulo, SP, Brazil*
[3]*Department of Physics, Lady Brabourne College, P1/2 Surawardi Avenue, Calcutta-700017, India*
(Received 20 October 2006; revised manuscript received 5 January 2007; published 12 April 2007)

We investigate Bose-Einstein condensates (BEC) containing a large number of bosonic atoms interacting via a finite-range semirealistic interatomic interaction. Ground state properties for an increasing number of atoms in the condensate have been calculated using a modification of the potential harmonic expansion method (including a short range correlation function in the expansion basis) to solve the many-body Schrödinger equation. An improved numerical algorithm for the calculation of the potential matrix elements permits us to have up to 14 000 atoms in the condensate. Although our approach is approximate and justified for dilute condensates, our results agree well with available diffusion Monte Carlo results for the same case. The ground state energies also agree well with those by the Gross-Pitaevskii equation method for up to 100 particles in the trap and become gradually larger than the latter (up to 5% for 14 000 atoms). The difference is attributed to the effects of finite range interatomic interaction and two-body correlations. Our approach presents a clear physical picture of the condensate, being computationally economical at the same time.

DOI: 10.1103/PhysRevA.75.042705 PACS number(s): 03.75.Hh, 31.15.Ja, 03.65.Ge, 03.75.Nt

I. INTRODUCTION

The theoretical investigation of Bose-Einstein condensates (BEC) has been a topic of increasing interest since the first experimental observation in supercooled trapped alkali atoms [1–3]. This constitutes a very difficult many-body problem. The ability to deal theoretically with a large collection of interacting particles is necessary for further progress. The number of interacting atoms in a typical experimentally achieved BEC is of the order of 10^3-10^6 [4]. An *ab initio* many-body approach to solve the Schrödinger equation for such a large number of interacting particles faces difficulties arising from too many degrees of freedom and too many pair-interaction bonds. Standard few body methods like hyperspherical harmonics method (HHM) [5], Faddeev [6] or Yakubovsky [7] equation methods are practical only for a few particles. An essentially exact result can be obtained by methods based on quantum Monte Carlo (QMC) procedure, viz., diffusion Monte Carlo (DMC) [8], variational Monte Carlo (VMC) [9], and Green's function Monte Carlo [10] methods. Although quite accurate solutions are possible, these methods demand a great deal of computation. Moreover, the computational requirements increase very rapidly as the number of atoms (A) increases. For this reason, the calculation by the DMC method has been reported in the literature only up to about $A=50$ [11]. More recently Purwanto and Zhang calculated column density up to 1000 trapped bosons by the ground state auxiliary-field quantum Monte Carlo method, while detailed properties were calculated for 100 trapped bosons [12]. Alternative procedures are thus important. For an *ab initio* but computationally simpler treatment of BEC, we have utilized the potential harmonic (PH) expansion method [13], which was originally proposed by Fabre [14] for nuclear systems. The PH expansion method (PHEM) is an approximate form of HHM where the principal assumption is the absence of higher-than-two-body correlations in the many-body wave function. Typical BEC, where the atomic cloud is required to be extremely dilute to avoid three- and higher-body collisions leading to recombination and consequent depletion of the condensate [4], is thus an ideal system for which this assumption is manifestly valid. In our earlier studies [15,16] we found that the PHEM results compare very well with DMC results even for strongly interacting BEC for $A \leqslant 50$. However, numerical difficulties did not allow the method to be applied to more than about 50 particles. The main difficulty was the evaluation of the potential matrix element

$$V_{KK'}(r) = (h_K^{\alpha\beta} h_{K'}^{\alpha\beta})^{-1/2} \int_{-1}^{+1} P_K^{\alpha\beta}(z) V\left(r\sqrt{\frac{1+z}{2}}\right) \times P_{K'}^{\alpha\beta}(z) w_l(z) dz, \tag{1}$$

where $V(r_{ij})$ is the two-body potential for the relative separation $r_{ij}\left(=r\sqrt{\frac{1+z}{2}}\right)$ of the interacting ijth pair, $P_K^{\alpha\beta}(z)$ is a Jacobi polynomial and its weight function and norm are $w_l(z) = (1-z)^{\alpha}(1+z)^{\beta}$ and $h_K^{\alpha\beta}$, respectively [17]. Now $\alpha[=(3A-8)/2]$ increases rapidly with A, while $\beta=l+1/2$ (l being the orbital angular momentum of the system) remains constant. For large A, $w_l(z)$ increases very rapidly from zero at $z=-1$ to a maximum of the order of 2^{α} at $z_m=\frac{\beta-\alpha}{\beta+\alpha}$; then within a small range of z-values it decreases rapidly and becomes vanishingly small for larger values of z. Although the factor 2^{α} cancels with the normalization factor $(h_K^{\alpha\beta} h_{K'}^{\alpha\beta})^{-1/2}$, the major contribution to $V_{KK'}(r)$ comes from a very narrow region near the lower limit of integration. This region shrinks rapidly as A (and hence α) increases. Then $V_{KK'}(r)$ for a short range potential practically vanishes (for relevant values of r) when evaluated numerically using any standard quadrature. This is so because the narrow contributing region is not well-represented unless an extremely large number of points

is used in the quadrature, which increases the CPU time enormously. Furthermore, the cumulative rounding off error also increases with the number of quadrature points. Thus using standard quadratures, $V_{KK'}(r)$ practically vanishes for $A>50$. Consequently the effect of two-body interaction is totally lost and the results reflect only the external confining potential. We have solved this difficulty [18] by splitting the integral in Eq. (1) into n subintegrals of gradually increasing intervals, h_0, ah_0, $a^2h_0,\ldots$, $a^{n-1}h_0$ and using a 32-point Gauss-Legendre quadrature [19] for each subintegral. The first subinterval h_0 can be made desirably small by choosing a fairly large. We have demonstrated [18] that $V_{KK'}(r)$ converges rapidly as n or a increases. With $a=5$ and $n=20$, one gets sufficiently converged (up to nine significant digits) results even for $A=15\,000$. With this method the PHEM can be used for systems containing quite large values of A. We have succeeded in calculating the properties of the condensate containing up to 14 000 trapped interacting bosons by the PHEM. The number is at least one order of magnitude larger than that reported in the literature by the QMC methods. Furthermore, we can include a realistic two-body interaction, e.g., van der Waals interaction (with a hard core) or Lennard-Jones interatomic potentials. The zero energy two-body wave function generated by such a potential is used as a short range correlation function in the potential harmonic expansion to enhance the rate of convergence of the PH expansion. While the computational requirements for an accurate calculation by the QMC methods are considerably costly, those for our procedure are very moderate. Even though the PHEM is an approximate solution of the many-body problem, the fact that our results compare quite well with the essentially exact QMC results indicates that the basic assumption, viz., absence of more-than-two-body correlations in the many-body wave function is well-justified, even for a strongly interacting BEC. In this paper, we present the results of our calculation for condensates containing up to 14 000 trapped ^{87}Rb and ^{23}Na atoms interacting via a short range repulsive potential and compare them with DMC and Gross-Pitaevskii (GP) results.

The paper is organized as follows: In Sec. II we briefly recapitulate the potential harmonics expansion method including a short range two-body correlation function. In Sec. III we present our numerical procedure, while the results appear in Sec. IV. Finally we draw our conclusions in Sec. V.

II. THEORETICAL FRAMEWORK

A. Expansion in potential harmonics basis

The mathematical details of the potential harmonics expansion method can be found in Ref. [14]. We briefly recapitulate it here. The Schrödinger equation for a system of A identical bosons (each of mass m), confined by an externally applied trapping potential V_{trap} and interacting via a two-body potential $V(\vec{x}_i-\vec{x}_j)$, is

$$\left[-\frac{\hbar^2}{2m}\sum_{i=1}^{A}\nabla_i^2+\sum_{i=1}^{A}V_{trap}(\vec{x}_i)+\sum_{ij>i}^{A}V(\vec{x}_i-\vec{x}_j)-E\right]\times\psi(\vec{x}_1,\ldots,\vec{x}_A)=0, \tag{2}$$

where $\vec{x}_i$ is the position coordinate of the ith particle. With the introduction of $N(=A-1)$ Jacobi vectors

$$\vec{\zeta}_i=\sqrt{\frac{2i}{i+1}}\left(\vec{x}_{i+1}-\frac{1}{i}\sum_{j=1}^{i}\vec{x}_j\right)\quad(i=1,\ldots,N) \tag{3}$$

and the center of mass vector $(\vec{R})$, the center of mass motion is separated and the relative motion is described by

$$\left[-\frac{\hbar^2}{m}\sum_{i=1}^{N}\nabla_{\vec{\zeta}_i}^2+V_{trap}+\sum_{ij>i}^{N}V_{ij}-E_R\right]\psi(\vec{\zeta}_1,\ldots,\vec{\zeta}_N)=0, \tag{4}$$

where E_R is the energy of the relative motion. Note that the labeling of the particle indices (and hence the Jacobi vectors) is arbitrary. A particular choice is obtained by renaming the relative separation $(\vec{r}_{ij})$ of the (ij)-interacting pair as $\vec{\zeta}_N$, whose polar coordinates are (θ,φ). We next define the hyperradius (r) of the set of A particles through [20]

$$r^2=\sum_{i=1}^{N}\zeta_i^2=\frac{2}{A}\sum_{i,j>i}^{A}r_{ij}^2=2\sum_{i=1}^{A}r_i^2, \tag{5}$$

where $\vec{r}_i$ is the coordinate of the ith particle from the center of mass of the system. The hyper-radius of the $(A-2)$ noninteracting particles is

$$\rho_{ij}=\left[\sum_{i=1}^{N-1}\zeta_i^2\right]^{1/2} \tag{6}$$

so that $r^2=\rho_{ij}^2+r_{ij}^2$. We introduce the hyperangle ϕ such that $r_{ij}=r\cos\phi$ and $\rho_{ij}=r\sin\phi$. Besides r, ϕ, θ, and φ, the remaining $(3N-4)$ variables of $(\vec{\zeta}_1,\ldots,\vec{\zeta}_{N-1})$ are collectively denoted by $\Omega_{N-1}^{(ij)}$ and are called hyperangles in $3(N-1)$ dimensional space when $\vec{\zeta}_N=\vec{r}_{ij}$. These are constituted by $2(N-1)$ polar angles associated with $\{\vec{\zeta}_1,\ldots,\vec{\zeta}_{N-1}\}$ and $(N-2)$ angles defining their relative lengths. The Laplace operator associated with the full set of N Jacobi vectors (which is proportional to the kinetic energy operator of the relative motion) is [20]

$$\nabla^2\equiv\sum_{i=1}^{N}\nabla_{\zeta_i}^2=\frac{\partial^2}{\partial r^2}+\frac{3A-4}{r}\frac{\partial}{\partial r}+\frac{L^2(\Omega_N)}{r^2}, \tag{7}$$

where $L^2(\Omega_N)$ is the grand orbital operator in $3N$-dimensional hyperangular space and has the form

$$L^2(\Omega_N)=4(1-z^2)\frac{\partial^2}{\partial z^2}+6[2-N(1+z)]\frac{\partial}{\partial z}+2\frac{l^2(\omega_{ij})}{1+z}+2\frac{L^2(\Omega_{N-1}^{(ij)})}{1-z}, \tag{8}$$

where $z=\cos 2\phi$, $\omega_{ij}\equiv(\theta,\varphi)$, and $L^2(\Omega_{N-1}^{(ij)})$ is the grand orbital operator in $3(N-1)$ dimensional space.

Splitting ψ of Eq. (4) in Faddeev components

$$\psi=\sum_{ij>i}^{A}\phi_{ij}, \tag{9}$$

Eq. (4) can be written as

$$[T + V_{trap} - E_R]\phi_{ij} = -V(r_{ij}) \sum_{kl>k}^{A} \phi_{kl}, \tag{10}$$

where $T = -\frac{\hbar^2}{m}\Sigma_{i=1}^{N}\nabla_{\vec{\zeta}_i}^2$. Applying $\Sigma_{ij>i}^{A}$ on both sides of Eq. (10), one gets back Eq. (4). The assumption that correlations higher than two-body ones in ψ are negligible, and that the angular and hyperangular momenta of the system are contributed by the interacting pair only, makes the Faddeev component ϕ_{ij} independent of the coordinates of all the particles other than the interacting pair [13,14], i.e., $\phi_{ij} = \phi_{ij}(\vec{r}_{ij}, r)$. With this assumption, $\phi_{ij}(\vec{r}_{ij}, r)$ can be expanded in the subset of hyperspherical harmonics necessary for the expansion of $V(\vec{r}_{ij})$. This subset of HH is called potential harmonics and is denoted by $\{\mathcal{P}_{2K+l}^{lm}(\Omega_N^{(ij)})\}$. Note that $\mathcal{P}_{2K+l}^{lm}(\Omega_N^{(ij)})$ depends only on $\vec{r}_{ij}$, i.e., $\vec{\zeta}_N$ and is independent of $(\vec{\zeta}_1, \ldots, \vec{\zeta}_{N-1})$. Thus

$$\phi_{ij}(\vec{r}_{ij}, r) = r^{-[(3N-1)/2]} \sum_K \mathcal{P}_{2K+l}^{lm}(\Omega_N^{(ij)}) u_K^l(r). \tag{11}$$

Here $\Omega_N^{(ij)}$ denotes the full set of hyperangles in $3N$-dimensional space for the choice $\vec{\zeta}_N = \vec{r}_{ij}$. The orbital angular momenta of the condensate and its projection are denoted by l and m, respectively. Since $\mathcal{P}_{2K+l}^{lm}(\Omega_N^{(ij)})$ is independent of $(\vec{\zeta}_1, \ldots, \vec{\zeta}_{N-1})$, it corresponds to zero eigenvalue of $L^2(\Omega_{N-1}^{(ij)})$. Closed analytic expression for $\mathcal{P}_{2K+l}^{lm}(\Omega_N^{(ij)})$ can be found in Ref. [14]. Substitution of Eq. (11) in Eq. (10) and projection on a particular PH gives

$$\left[-\frac{\hbar^2}{m}\frac{d^2}{dr^2} + V_{trap} + \frac{\hbar^2}{m}\frac{\mathcal{L}_\mathcal{K}(\mathcal{L}_\mathcal{K}+1)}{r^2} - E_R\right] u_K^l(r) + \sum_{K'} f_{K'l}^2 V_{KK'}(r) u_{K'}^l(r) = 0, \tag{12}$$

where

$$\mathcal{L}_\mathcal{K} = 2K + l + \frac{3N-3}{2},$$

$$f_{Kl}^2 = \sum_{k,l>k} \langle \mathcal{P}_{2K+l}^{lm}(\Omega_N^{(ij)}) | \mathcal{P}_{2K+l}^{lm}(\Omega_N^{(kl)}) \rangle. \tag{13}$$

An analytic expression for f_{Kl}^2 is given in Ref. [13]. In the present work, we take V_{trap} as a spherically symmetric harmonic oscillator potential, $V_{trap} = \Sigma_{i=1}^{A} \frac{1}{2} m\omega^2 r_i^2 = \frac{1}{4} m\omega^2 r^2$. This is hypercentral and is very simple to include in Eq. (12). However, most experimental setups have axially symmetric harmonic traps. In recent experiments rotating traps have been used [21] for which asymmetric or anharmonic confining potential is important. For an arbitrary fully asymmetric trap, Eq. (5) cannot be used and the present choice of Jacobi coordinates is not profitable. For a harmonic trap with different confinement frequencies in the three Cartesian directions, one can take Cartesian components of Eq. (3) and introduce three *unphysical* variables through $r_k^2 = \Sigma_{i=1}^{N} \zeta_{ik}^2$, ζ_{ik} being the kth Cartesian component $(k = x, y, z)$ of $\vec{\zeta}_i$. The above procedure will then result in an equation similar to Eq. (12), but much more difficult to handle. For simplicity and to study the basic properties, we restrict ourselves to spherical traps.

The potential matrix element is

$$V_{KK'}(r) = \int \mathcal{P}_{2K+l}^{lm*}(\Omega_N^{(ij)}) V(r_{ij}) \mathcal{P}_{2K'+l}^{lm}(\Omega_N^{(ij)}) d\Omega_N^{(ij)}$$
$$= (h_K^{\alpha\beta} h_{K'}^{\alpha\beta})^{-1/2} \int_{-1}^{+1} P_K^{\alpha\beta}(z) V\left(r\sqrt{\frac{1+z}{2}}\right) \times P_{K'}^{\alpha\beta}(z) w_l(z) dz, \tag{14}$$

Eq. (12) can be put in a symmetric form by multiplying it by the constant f_{Kl} [13],

$$\left[-\frac{\hbar^2}{m}\frac{d^2}{dr^2} + V_{trap} + \frac{\hbar^2}{mr^2}\{\mathcal{L}(\mathcal{L}+1) + 4K(K+\alpha+\beta+1)\} - E_R\right] U_{Kl}(r) + \sum_{K'} \bar{V}_{KK'}(r) U_{K'l}(r) = 0, \tag{15}$$

where $\mathcal{L} = l + (3A-6)/2$ and

$$\bar{V}_{KK'}(r) = f_{Kl} V_{KK'}(r) f_{K'l},$$
$$U_{Kl}(r) = f_{Kl} u_K^l(r). \tag{16}$$

We solve Eq. (15) numerically to obtain the energy and wave function of the condensate.

B. Incorporation of *s*-wave scattering length for a finite range interatomic potential

In a typical BEC achieved in laboratories, the average interparticle separation is much larger than the range of two-body interaction. This is necessary to prevent three- and higher-body collisions, which would give rise to molecule formation and eventual depletion of the BEC. Under these conditions, the two-body interaction can be represented by the s-wave scattering length (a_s). Assumption of a contact interaction (valid only in a dilute BEC, where the range of two-body interaction is negligible compared to the average interparticle separation) gives rise to the mean-field Gross-Pitaevskii (GP) equation [4]. In the original BEC with ^{87}Rb [3] and ^{23}Na atoms [22], a_s had positive values representing repulsive effective interaction. However, a realistic interatomic interaction is always attractive at larger separations. An attractive potential normally gives negative a_s; it can give a positive a_s if the zero energy two-body wave function in this potential has one or more nodes. The asymptotic part of the zero energy two-body wave function $\eta(r_{ij})$, for the potential $V(r_{ij})$, has the form $(c_1 r_{ij} + c_2)$ and the corresponding scattering length is given by $a_s = -\frac{c_2}{c_1}$. Relatively small changes in the short range part of $V(r_{ij})$ can introduce one or more nodes near the origin in $\eta(r_{ij})$. This in turn drastically alters the asymptotic linear part. Consequently the value of a_s can change enormously. In the laboratory, the scattering length can be tuned using Feshbach resonances [23]. The energy scale for the kinetic energy of the interacting pair is the oscillator energy ($\hbar\omega$) scale. In laboratory BECs this is extremely small ($\sim 10^{-13}$ eV) compared to atomic energy scale (~ 1 eV). Thus for the Faddeev component ϕ_{ij} of the

condensate wave function, the kinetic energy of the interacting pair is negligibly small compared to atomic interaction $V(r_{ij})$ and for $r_{ij}\to 0$, ϕ_{ij} is well-represented by $\eta(r_{ij})$. Thus $\eta(r_{ij})$ is an accurate representation of the two-body pair correlation for interatomic separations at the atomic length scale. Since the potential harmonic $\mathcal{P}^{lm}_{2K+l}(\Omega^{(ij)}_N)$ is finite for $r_{ij}\to 0$, the rate of convergence of the PH expansion of Eq. (11) will be very slow. To enhance the rate of convergence, we use $\eta(r_{ij})$ as a short-range correlation function (corresponding to the appropriate scattering length) in the PH expansion and replace Eq. (11) by

$$\phi_{ij}(\vec{r}_{ij},r) = r^{-[(3N-1)/2]}\sum_K \mathcal{P}^{lm}_{2K+l}(\Omega^{(ij)}_N)\,\eta(r_{ij})u^l_K(r). \quad (17)$$

Inclusion of $\eta(r_{ij})$, in effect, constrains the motion of individual atoms to follow the dictate of a particular scattering length. In practice, we solve the zero energy two-body wave function $\eta(r_{ij})$ in the chosen two-body potential $V(r_{ij})$ such that a_s has the desired value. The correlation function is chosen to satisfy the appropriate healing condition, viz., approaching unity for large r_{ij} as in Ref. [24]. Inclusion of $\eta(r_{ij})$ introduces correction terms in Eq. (15). However, such correction terms are quite negligible for a typical laboratory BEC. This is because the relevant value of r (which is the position of the minimum of the effective potential in which the condensate moves) is typically $\sim 10-100$ oscillator units (o.u.) and is much larger than the healing distance ($\sim$range of two-body interaction). This $\eta(r_{ij})$ is then used in Eq. (17). As a result the potential matrix element becomes

$$V_{KK'}(r) = (h^{\alpha\beta}_K h^{\alpha\beta}_{K'})^{-1/2}\int_{-1}^{+1} P^{\alpha\beta}_K(z)V\left(r\sqrt{\frac{1+z}{2}}\right)P^{\alpha\beta}_{K'}(z) \times \eta\left(r\sqrt{\frac{1+z}{2}}\right)w_l(z)dz. \quad (18)$$

Thus even an attractive $V(r_{ij})$ can contribute positively to $V_{KK'}(r)$ if $\eta(r_{ij})$ is also negative over a significant interval of r_{ij}. Inclusion of $\eta(r_{ij})$ has the additional advantage of enhancing the rate of convergence of the PH expansion, since it correctly reproduces the short separation two-body correlation of the many-body wave function.

III. NUMERICAL PROCEDURE

A. Accurate evaluation of $V_{KK'}(r)$

Although the procedure outlined in Sec. II A is, in principle, appropriate for a dilute BEC, there are certain difficulties. The basic length scale for a harmonic oscillator trap of circular frequency ω is $a_{ho}=\sqrt{\frac{\hbar}{m\omega}}$, which for a typical experimental setup, is of the order of 10^4 Bohr. The effective potential in hyperradial space due to the hypercentrifugal repulsion together with the harmonic oscillator trap has a minimum at about $\sqrt{3A}a_{ho}$. Thus minimum of the effective potential for a dilute condensate, with $A\sim 10^4$ will be at $\sim 10^6$ Bohr, which is $\sim 10^5$ times larger than the typical range of the interatomic interaction. This means that almost the entire contribution to $V_{KK'}(r)$ from the integral in Eq. (18), for such a typical case, comes from a very narrow interval ($\sim 10^{-10}$) of z near the lower limit of integration. Furthermore, $w_l(z)$ shoots up from zero at $z=-1$ to a maximum $\sim 2^\alpha$ at $z_m=\frac{\beta-\alpha}{\beta+\alpha}$ and then decreases rapidly reaching a value of about 10^{-10} of the peak value at $z\approx -1+0.003$. Although the peak value 2^α is extremely large for large A, it cancels with the same factor in $(h^{\alpha\beta}_K h^{\alpha\beta}_{K'})^{-1/2}$ (see Ref. [17]). Thus for large A, not only is the contributing interval of z very narrow, but also the integrand varies enormously within this narrow interval. Any standard quadrature to evaluate the integrand in Eq. (18) thus gives practically zero for $A>50$, since very few points will be within this critical range, unless an extremely large-point quadrature is used, which would require an enormously large CPU time. This was the reason why we could not go beyond $A=50$ in our earlier attempts [13,15,16]. We have solved this problem by splitting the interval $[-1,1]$ of integration into n gradually increasing subintervals [18]: h_0, ah_0, $a^2h_0,\ldots,a^{n-1}h_0$, such that

$$h_0 + ah_0 + a^2h_0 + \cdots + a^{n-1}h_0 = 2. \quad (19)$$

From this we have

$$h_0 = \frac{2(a-1)}{(a^n-1)} \quad (20)$$

and the integral in Eq. (18) is replaced by a sum of n subintegrals

$$\int_{-1}^{1} = \int_{-1}^{-1+h_0} + \int_{-1+h_0}^{-1+h_0+ah_0} + \cdots + \int_{1-a^{n-1}h_0}^{1}. \quad (21)$$

Each subintegral is evaluated by a 32-point Gauss-Legendre quadrature [19]. With an appropriate choice of a, the first subinterval h_0 can be made desirably small, even for a relatively small value of n. For example, if we fix $n=20$, then for $a=2$, $h_0\simeq 2\times 10^{-6}$ while for $a=5$, h_0 becomes $\sim 10^{-14}$. Thus the integral can be evaluated accurately without appreciable increase in CPU time. We have shown [18] that the choice $n=20$, $a=5$ is sufficient to evaluate $V_{KK'}(r)$ for A up to 15 000 with an accuracy of one part in 10^9.

B. Solution of coupled differential equation

Restricting the K-sum in Eq. (17) to an upper limit of K_{max} (which is determined from the requirement of convergence), we solve the set of coupled differential equations (CDE), Eq. (15), by hyperspherical adiabatic approximation (HAA) [25]. Assuming that the hyperradial motion is slow compared to the hyperangular motion, the latter is separated adiabatically and solved for a fixed value of r. This is achieved by diagonalizing the potential matrix $[V_{KK'}(r)]$ plus the diagonal hypercentrifugal term of Eq. (15) for a fixed value of r. The lowest eigenvalue, $\omega_0(r)$, gives the effective potential (as a parametric function of r) in which the condensate moves [13]. In the uncoupled adiabatic approximation, an overbinding correction term is also included with $\omega_0(r)$ [25]:

TABLE I. Results for ^{87}Rb using $V_0\,\mathrm{sech}^2\,(r_{ij}/r_0)$ potential for $a_s=0.004\,33$. All results are given in oscillator units (o.u.).

A	Interaction energy $\langle V\rangle$	Kinetic energy $\langle T\rangle$	Trap energy $\langle V_{trap}\rangle$	Total ground state energy (E) PHEM	Total ground state energy (E) DMC Ref. [11]	r_{av} (of PHEM)	r_{rms}^{GP} (of GP)
3	0.0010	3.0015	1.5077	4.5103	4.51037	1.003	1.228
5	0.0151	4.4888	3.0322	7.5360	7.53439	1.101	1.230
10	0.1257	8.1614	6.8619	15.1490	15.1539	1.171	1.235
20	0.5831	15.324	14.714	30.6209	30.639	1.213	1.245
50	3.6395	35.617	39.614	78.8704		1.259	1.272
100	13.492	66.285	85.130	164.907		1.305	1.311
500	220.00	245.23	574.85	1040.09		1.516	1.510
1000	660.02	404.05	1395.0	2459.11		1.670	1.654
5000	7260.6	1166.6	12068	20495.4		2.197	2.151
10000	19659	1798.1	31309	52765.2		2.502	2.440
14000	31751	2212.4	49868	83830.9		2.669	2.599

$$\left[-\frac{\hbar^2}{m}\frac{d^2}{dr^2}+\omega_0(r)+\sum_{K=0}^{K_{max}}\left|\frac{d\chi_{K0}(r)}{dr}\right|^2-E_R\right]\zeta_0(r)=0, \tag{22}$$

where $\chi_{K0}(r)$ is the Kth element of the column vector corresponding to the lowest eigenvalue $\omega_0(r)$. Equation (22) is solved by the standard Runga-Kutta algorithm [19], subject to appropriate boundary conditions for $r\to 0$ and $r\to\infty$, for the relative energy E_R and the wave function $\zeta_0(r)$. The total energy E of the condensate is obtained by adding the center of mass energy to E_R. The partial wave $U_{Kl}(r)$ is given in HAA by [25]

$$U_{Kl}(r)\simeq\zeta_0(r)\chi_{K0}(r). \tag{23}$$

Although Eq. (15) can be solved by an exact numerical algorithm, e.g., the renormalized Numerov method [26], we prefer HAA for reasons of computational economy. Earlier works demonstrated that the HAA results agree very well with exact ones for both atomic [27–29] and nuclear [30,31] cases.

IV. RESULTS AND DISCUSSIONS

A. Choice of potential

We choose a finite range semirealistic potential of the form

$$V(r_{ij})=V_0\,\mathrm{sech}^2\left(\frac{r_{ij}}{r_0}\right), \tag{24}$$

whose range (r_0) and strength (V_0) can be adjusted to give the experimental s-wave scattering length (a_s). The potential is uniformly attractive or repulsive accordingly as V_0 is negative or positive, respectively. The advantage of this choice is that this potential is smooth and the range can be chosen to be of the order of atomic interaction range. Since $a_{ho}\sim 10^{-4}$ cm, we choose $r_0=10^{-3}$ o.u. Then the zero energy two-body Schrödinger equation is solved to obtain the asymptotic solution. This has the form $c_1 r_{ij}+c_2$ in the potential free region, so that $a_s=-\frac{c_2}{c_1}$. The strength V_0 is then adjusted to get the experimental value of a_s.

B. Results for ^{87}Rb

As an example, we consider the BEC experiment with ^{87}Rb atoms at the Joint Institute for Laboratory Astrophysics (JILA) [3], for which $a_s=0.004\,33$ o.u. [11]. This gives $V_0=1.818\,47\times 10^9$ o.u. for $r_0=10^{-3}$ o.u. Calculated ground state energy (E) for several representative number of atoms (A) in the trap are presented in the fifth column of Table I. Our results agree fairly well with the energies calculated by Blume and Greene [11] using the DMC method (also quoted in Table I), as also with our previous calculation [15], for the available A values. Since DMC results are not available for $A>20$, we compare our results graphically with the GP results in Fig. 1, where ground state energy per particle of the condensate calculated by the GP equation is plotted against A (in log scale). We use a logarithmic scale for A, in order that points corresponding to smaller A values can be distin-

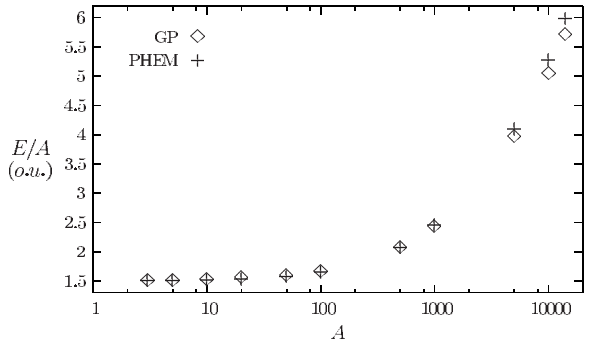

FIG. 1. Comparison of ground state energy per particle by PHEM and GP for ^{87}Rb using $V_0\,\mathrm{sech}^2(r_{ij}/r_0)$ potential. Note the logarithmic scale for the number of particles in the condensate.

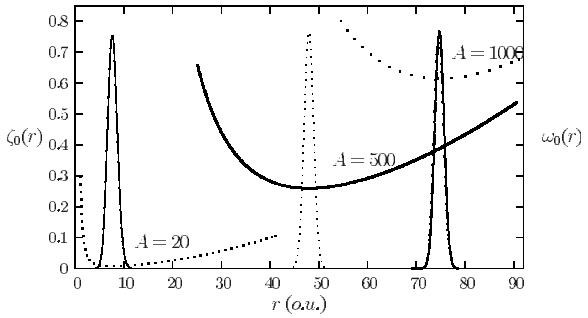

FIG. 2. Plot of wave function $\zeta_0(r)$ (vertical peaks) and the lowest eigenpotential $\omega_0(r)$ as a function of hyper-radius for 20, 500, and 1000 atoms of ^{87}Rb. The actual value of $\omega_0(r)$ can be obtained by multiplying the vertical scale by 4000.0. The peak of the wave function occurs at the position of the minimum of lowest eigenpotential.

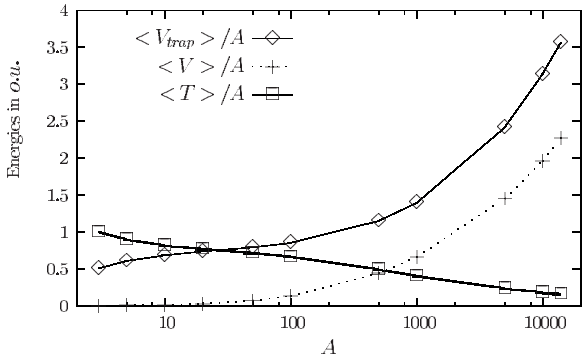

FIG. 3. Plot of $\langle V_{trap}\rangle$, $\langle V\rangle$, and $\langle T\rangle$ per particle as a function of the number of particles A for ^{87}Rb (a_s=0.004 33 o.u.). Note that the calculated points are joined by lines to guide the eye.

guished. Consequently the E/A versus A curve looks different from the usual linear A plot. In Fig. 1 we also plot the same quantity calculated by the PHEM method. One notices that the agreement is quite good up to $A=100$. The difference increases as A increases but remains within 5% even for $A=14\,000$. One can also notice that the PHEM energy is larger than the GP energy. This indicates the effect of interatomic interaction and correlations present in the PHEM. By contrast, the GP equation comes from the mean field theory which includes no correlation and uses only two-body zero range interaction. The effective potential in the PHEM has contributions from the trapping potential, hypercentrifugal repulsion (HCFR), and the total two-body interaction (TTBI), which are, respectively, the second, third, and the last term of Eq. (15). While strength of V_{trap} is independent of $A\left(=\frac{1}{4}m\omega^2r^2\right)$, strength of HCFR increases roughly as A^2 for large A. Although $V(r_{ij})$ is independent of A, the number of binary bonds also increases roughly as A^2; hence TTBI (which is repulsive in our present study) also increases roughly as A^2. Both HCFR and TTBI will push the particles outwards, forcing them to climb the outer wall of V_{trap}, the effect increases as A increases. While V_{trap} increases steadily $(\propto r^2)$ as r increases in the same manner for all A, both HCFR and TTBI decrease with increasing r (the former as $\frac{1}{r^2}$), but their strengths increase approximately as A^2. Consequently $\omega_0(r)$ is flatter near its minimum for smaller A. As A increases, HCFR plus TTBI decrease more stiffly as r increases. Hence $\omega_0(r)$ becomes less flat near its minimum whose position shifts to larger r. This is shown in Fig. 2 for three representative values of A (20, 500, and 1000), in which the ground state wave function $[\zeta_0(r)]$ is also plotted. Furthermore, the net effect of V_{trap}, HCFR and TTBI increase the ground state energy of the condensate rapidly as A increases. This explains the gradual increase of the difference of PHEM and GP energies as A increases.

In Table I, we also present calculated expectation values of interaction ($\langle V\rangle$), kinetic ($\langle T\rangle$), and trap ($\langle V_{trap}\rangle$) energies of all the particles in the spherically symmetric harmonic trap in the second, third, and fourth columns, respectively. The expectation value of the interaction energy is obtained as the expectation value of $\Sigma_{ij>i}^{A}V(r_{ij})$ in the ground state. Purwanto and Zhang [12] presented detailed results by the auxiliary-field quantum Monte Carlo method for $A=100$ only. Our choice of the experimental a_s corresponds to the lowest value of the range of a_s values chosen by them. Al-

TABLE II. Results for ^{23}Na using $V_0\,\mathrm{sech}^2\,(r_{ij}/r_0)$ potential for a_s=0.002 84. All results are given in oscillator units (o.u.).

A	Interaction energy $\langle V\rangle$	Kinetic energy $\langle T\rangle$	Trap energy $\langle V_{trap}\rangle$	Total ground state energy by PHEM E	r_{av} (of PHEM)	r_{rms}^{GP} (of GP)
3	0.0005	3.0013	1.5047	4.50660	1.001	1.227
5	0.0099	4.4913	3.0235	7.52472	1.100	1.228
10	0.0831	8.1917	6.8233	15.0981	1.168	1.232
20	0.3884	15.466	14.556	30.4108	1.206	1.238
50	2.4743	36.448	38.665	77.5873	1.244	1.257
100	9.4186	69.030	81.660	160.109	1.278	1.285
500	167.67	270.60	520.60	958.863	1.443	1.440
1000	520.59	456.01	1235.4	2212.00	1.572	1.561
5000	6004.9	1358.1	10364	17726.8	2.036	1.997
10000	16413	2106.2	26724	45243.7	2.312	2.258
14000	26591	2596.7	42482	71670.0	2.463	2.402

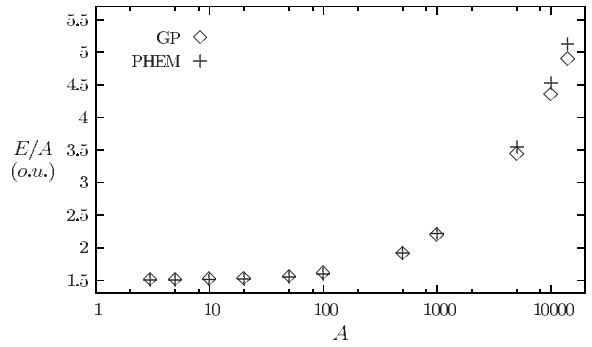

FIG. 4. Comparison of ground state energy per particle by PHEM and GP equation for ^{23}Na using $V_0\,\mathrm{sech}^2(r_{ij}/r_0)$ potential.

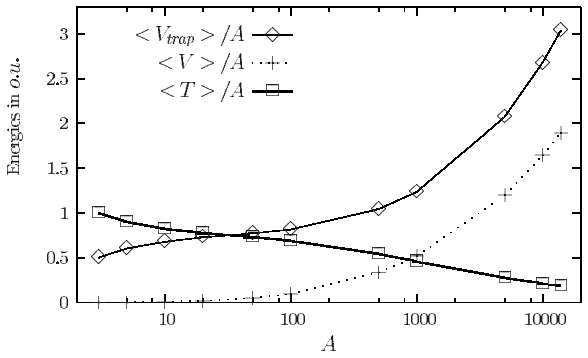

FIG. 5. Plot of $\langle V_{trap}\rangle$, $\langle V\rangle$, and $\langle T\rangle$ per particle as a function of the number of particles A for ^{23}Na (a_s=0.002 84 o.u.). Note that the calculated points are joined by lines to guide the eye.

though no numerical values were given, from Fig. 3 of Ref. [12], it appears that E/A, $\langle V\rangle/A$, $\langle V_{trap}\rangle/A$, and $\langle T\rangle/A$ calculated by us agree fairly well with those calculated by Purwanto and Zhang for the same value of a_s. One notices from Table I that the interaction energy per binary bond $[2\langle V\rangle/A(A-1)]$ is a slowly varying function of A. It increases initially for small A, then attains a maximum at $A \approx 20$, then decreases very slowly for larger values of A. This is in agreement with our expectation. We already noticed that $\langle V\rangle$ increases with the number of bonds. Hence interaction energy per bond may be expected to be approximately constant. It is not exactly a constant, since the average interparticle separation changes with A. For very large values of A, the interparticle separation faces a competition between two opposing effects: more particles squeeze within the trap (tending to reduce average separation) and the rapidly increasing mutual repulsion (tending to increase average separation). Hence the number density in physical space increases slowly with A (approximately as $A^{2/5}$ for large A), as can be seen from the values of r_{av} presented in Table I (see below). As a result, interaction energy per bond increases initially, then changes very slowly for larger A. We plot $\langle V\rangle/A$, $\langle V_{trap}\rangle/A$, and $\langle T\rangle/A$ against A for ^{87}Rb in Fig. 3. The trap energy per particle increases gradually, since the increasing mutual repulsion with increasing A pushes the particles outward, forcing them to climb the hill of V_{trap}. This is seen in Fig. 3. Figure 3 also shows that $\langle T\rangle/A$ decreases gradually as A increases. As A increases, the region of hyperspace available for the motion of atoms increases. Consequently kinetic energy per atom decreases, although the total kinetic energy of all atoms in the trap increases slowly (Table I).

In the last column of Table I, we present the rms separation from the center (r_{rms}^{GP}) by the GP equation. By contrast the rms hyper-radius by the PHEM has much larger values (see Fig. 2). This is understandable, since the hyper-radius is a length variable in the hyperspace and is not directly related to physical separations. From Eq. (5) one notices that the hyper-radius increases rapidly as the number of particles increases. However, Eq. (5) also shows that the average square of distance of individual particles from the center of mass $\left(=\frac{1}{A}\sum_{i=1}^{A} r_i^2\right)$ is directly related to the square of the hyper-radius $\left(=\frac{r^2}{2A}\right)$. Hence we define an average physical size of the condensate as

$$r_{av} = \left[\frac{\langle r^2\rangle}{2A}\right]^{1/2}.$$

One can expect that r_{av} of PHEM should be comparable to r_{rms}^{GP} of the GP equation. In the seventh column of Table I we present r_{av} for the chosen values of A. It is seen that, although r_{av} is appreciably smaller than r_{rms}^{GP} for $A<20$, the difference decreases to a minimum for A in the range 100–500, and for larger A, r_{av} is larger than r_{rms}^{GP}, the difference being less than 3% even for $A=14\,000$. One can calculate the number density (n_d), assuming the particles to be distributed over a sphere of radius r_{av} in the physical space. Then one can see from Table I that n_d is approximately proportional to $A^{2/5}$ for $A>1000$, which agrees with the Thomas-Fermi approximation in the large A limit [4]. Note that the PHEM wave function $[\zeta_0(r)]$ is a function of the hyper-radius and hence cannot be compared with the GP wave function in the physical space. Thus we cannot compare the PHEM density profile with that by the GP method. Still the average physical size of the condensate and its number density agree fairly well with corresponding physical quantities by the GP equation method or the Thomas-Fermi approximation for large A.

C. Results for ^{23}Na

The results for ^{23}Na atoms in the experimental trap [22], with a_s=4.9 nm (corresponding to 0.002 84 o.u.), are presented in Table II. We tabulate the same quantities in the various columns as in Table I (no DMC results are available in this case). The ground state energy per particle by the PHEM method is compared with that by the GP equation method in Fig. 4. Once again the general feature is similar to that for ^{87}Rb. However, one can notice that the difference is larger for ^{87}Rb than for ^{23}Na. This is expected since a_s is smaller for ^{23}Na. In Fig. 5, we plot $\langle V\rangle/A$, $\langle V_{trap}\rangle/A$, and $\langle T\rangle/A$ for ^{23}Na. We again notice the same qualitative features as in the case of ^{87}Rb but less pronounced, as expected.

V. CONCLUSIONS

We have demonstrated that the correlated potential harmonics expansion method (which assumes that correlations higher than two-body ones are negligible in a dilute BEC),

together with an improved algorithm for the evaluation of the potential matrix elements, is a sufficiently accurate and computationally economical method for the study of BEC. The fact that the computed observables agree well with available quantum Monte Carlo results shows that the basic assumption is justified. The improved algorithm allows one to study condensates containing up to 14 000 atoms. This is at least an order of magnitude larger that the maximum number of atoms in the condensate reported so far by the essentially exact quantum Monte Carlo methods. We have calculated the ground state energy of the condensate, together with expectation values of kinetic, interaction, and trap energies. We also define and evaluate an average physical size (r_{av}) of the condensate. We have further compared our results with those by the GP equation method for the same value of the scattering length. The ground state energy per particle by the PHEM is very close to that by the GP equation for small A and the difference increases with A, reaching about a 5% increase for $A=14\,000$ for ^{87}Rb. The enhanced energy is due to the finite range interatomic interactions and two-body correlations. The rms radius of the condensate obtained by the GP equation compares fairly well with r_{av} calculated by PHEM except for $A<20$, indicating that the physical size of the condensate obtained by both the PHEM and GP equation are comparable, even for $A=14\,000$. Furthermore, the average interaction energy per binary bond is a slowly varying function (decreasing slowly for large A) of the number of atoms. This is understandable, since as more atoms are squeezed into the condensate, they face a stronger mutual repulsion and the number density increases approximately as $A^{2/5}$ for large A. As A increases, increased mutual repulsion and also the hypercentrifugal repulsion forces the system to climb the stiff walls of the confining potential. As a result, the expectation value of the trap energy per particle increases with A. Increase in available volume in the hyperspace reduces the average kinetic energy per particle, as A increases.

ACKNOWLEDGMENTS

This work has been partially supported by CNPq and FAPESP (Brazil) and Department of Science and Technology (DST, India). T.K.D. wishes to thank FAPESP (Brazil) for providing financial assistance for his visit to the Universidade de São Paulo, where part of this work was done. A.K. acknowledges DST (India).

[1] K. B. Davis, M.-O. Mewes, M. R. Andrews, N. J. van Druten, D. S. Durfee, D. M. Kurn, and W. Ketterle, Phys. Rev. Lett. **75**, 3969 (1995).
[2] C. C. Bradley, C. A. Sackett, J. J. Tollett, and R. G. Hulet, Phys. Rev. Lett. **75**, 1687 (1995).
[3] M. H. Anderson, J. R. Ensher, M. R. Matthews, C. E. Wieman, and E. A. Cornell, Science **269**, 198 (1995).
[4] F. Dalfovo, S. Giorgini, L. P. Pitaevskii, and S. Stingari, Rev. Mod. Phys. **71**, 463 (1999).
[5] J. L. Ballot and M. Fabre de la Ripelle, Ann. Phys. (N.Y.) **127**, 62 (1980).
[6] L. D. Faddeev, Zh. Eksp. Teor. Fiz. **39**, 1459 (1960) [Sov. Phys. JETP **12**, 1014 (1961)]; L. D. Faddeev, *Mathematical Aspects of the Three Body Problem in Quantum Scattering Theory* (translated from Russian), The Israel Program of Scientific Translations (Davey, New York, 1965).
[7] O. A. Yakubovsky, Yad. Fiz. **5**, 1312 (1967) [Sov. J. Nucl. Phys. **5**, 937 (1967)].
[8] D. M. Ceperley and B. J. Adler, Phys. Rev. Lett. **45**, 566 (1980); P. J. Reynolds, D. M. Ceperley, B. J. Adler, and W. A. Lester, J. Chem. Phys. **77**, 5593 (1982).
[9] J. L. DuBois and H. R. Glyde, Phys. Rev. A **63**, 023602 (2001).
[10] V. R. Pandharipande, J. G. Zabolitzky, S. C. Pieper, R. B. Wiringa, and U. Helmbrecht, Phys. Rev. Lett. **50**, 1676 (1983).
[11] D. Blume and C. H. Greene, Phys. Rev. A **63**, 063601 (2001).
[12] W. Purwanto and S. Zhang, Phys. Rev. A **72**, 053610 (2005).
[13] T. K. Das and B. Chakrabarti, Phys. Rev. A **70**, 063601 (2004).
[14] M. Fabre de la Ripelle, Ann. Phys. (N.Y.) **147**, 281 (1983).
[15] B. Chakrabarti, A. Kundu, and T. K. Das, J. Phys. B **38**, 2457 (2005).
[16] A. Kundu, B. Chakrabarti, and T. K. Das, Pramana **65**, 61 (2005).
[17] M. Abramowitz and I. A. Stegun, *Handbook of Mathematical Functions* (Dover, New York, 1972), p. 773.
[18] T. K. Das and S. Canuto (unpublished).
[19] W. H. Press*et al.*, *Numerical Recipies in Fortran* (Cambridge University Press, Cambridge, England, 1992).
[20] M. Fabre de la Ripelle, Few-Body Syst. **1**, 181 (1986).
[21] N. G. Parker and C. S. Adams, J. Phys. B **39**, 43 (2006); V. Bretin, S. Stock, Y. Seurin, and J. Dalibard, Phys. Rev. Lett. **92**, 050403 (2004); T. K. Ghosh, Eur. Phys. J. D **31**, 101 (2004).
[22] K. B. Davis, M.-O. Mewes, M. A. Joffe, M. R. Andrews, and W. Ketterle, Phys. Rev. Lett. **74**, 5202 (1995).
[23] C. J. Pethik and H. Smith, *Bose-Einstein Condensation in Dilute Gases* (Cambridge University Press, Cambridge, England, 2001).
[24] P. Barletta and A. Kievsky, Phys. Rev. A **64**, 042514 (2001).
[25] T. K. Das, H. T. Coelho, and M. Fabre de la Ripelle, Phys. Rev. C **26**, 2281 (1982).
[26] B. R. Johnson, J. Chem. Phys. **69**, 4678 (1978).
[27] V. P. Brito, H. T. Coelho, and T. K. Das, Phys. Rev. A **40**, 3346 (1989).
[28] R. Chattopadhyay and T. K. Das, Phys. Rev. A **56**, 1281 (1997).
[29] T. K. Das and B. Chakrabarti, Int. J. Mod. Phys. A **19**, 4973 (2004).
[30] T. K. Das, H. T. Coelho, and M. Fabre de la Ripelle, Phys. Rev. C **26**, 2288 (1982).
[31] M. A. Khan, T. K. Das, and B. Chakrabarti, Int. J. Mod. Phys. E **10**, 107 (2001).